Accepted for publication on 02/28/2012 in Optics Express

Optical microscope angular illumination analysis

Ravikiran Attota* and Richard Silver

Semiconductor and Dimensional Metrology Division, National Institute of Standards and Technology, Gaithersburg, MD 20899
*[*Corresponding author: ravikiran.attota@nist.gov*]*

Abstract
For high precision applications of optical microscopes, it is critical to achieve symmetrical angular illumination intensity at the sample plane, in addition to uniform spatial irradiance achieved by Köhler illumination. A correlation between the angular illumination asymmetry and the contrast in the image of a line grating target was demonstrated as the target is scanned through focus. Using this correlation, we present a novel, yet simple method of experimentally evaluating the **an**gular **il**lumination **as**ymmetry (ANILAS) at the sample plane of an optical microscope across the field of view. This ANILAS map is expected to be a useful method for assessing the illumination condition of optical systems.

© 2012 Optical Society of America

OCIS codes: (180.0180.) Microscopy; (220.4840.) Testing; (220.1140.) Alignment; (220.2945.) Illumination design;

References and links

1. A. Koehler, "New method of illumination for phomicrographical purposes," J. R. Micro. Soc., **14**, 261–262 (1894).
2. P.J. Evennett, "Köhler iIllumination centenary: a Collection of papers detailing Köhler illumination," R. Micro. Soc., 1–30 (1994).
3. C. Progler, H. Dua, and G. Wells, "Potential causes of across field CD variation," Proc. SPIE, **3051**, 660-671 (1997).
4. Y. Borodovsky, "Impact of local partial coherence variations on exposure tool performance," Proc. SPIE, **2440**, 750 –770 (1995).
5. J.P. Kirk and C.J. Progler, "Pupil illumination: in situ measurement of partial coherence," Proc. SPIE **3334**, 281-288 (1998).
6. K. Sato, S. Tanaka, T. Fujisawa, and S. Inoue, "Measurement of effective source shift using a grating-pinhole mask," Proc. SPIE **3679**, 99-107 (1999).
7. G. Zhang, C. Wang, C. L. Tan, J. R. Ilzhoefer, C. Atkinson, S. P. Renwick, S. D. Slonaker, D. Godfrey and C. H. Fruga, "Illumination pupil gill measurement and analysis and its application in scanner V-H bias characterization for 130nm node and beyond," Proc. SPIE **5040**-5, 45-56 (2003).
8. G. McIntyre and A.R. Neureuther, "Linear phase ring illumination monitor," J. Vac. Sci. Technol. B **21**, 2800-2805 (2003).
9. R.M. Silver, M. Stocker, R. Attota, M. Bishop, J. Jun, E., Marx, M. Davidson, and R. Larrabee, "Calibration strategies for overlay and registration metrology," Proc. SPIE, **5038**, 103 – 120 (2003).
10. J. Bendik, Y. Yamaguchia, L. G. Finknerb, and A. H. Smitha, "A simulation performance framework using in-situ metrology," Proc. SPIE, **5754**, 930-941 (2005).
11. Y.J. Sohn, B.M. Barnes, L. Howard, R.M. Silver, R. Attota, and M.T. Stocker, "Köhler illumination for high resolution optical metrology," Proc. SPIE, **6152**, 61523S (2006).

12. R.M. Silver, B.M. Barnes, R. Attota, J. Jun, M. Stocker,E. Marx, and H.J. Patrick, "Scatterfield microscopy for extending the limits of image-based optical metrology," Appl. Opt., **46**, 4248-4257 (2007).
13. M. Davidson, "Analytic waveguide solutions and the coherence probe microscope," Proc. Microcircuit Engg., **90**, Leuven, Belgium, September (1990).
14. E. Marx, "Images of strips on and trenches in substrates," Appl. Opt. **46**, 5571-5587 (2007).
15. R. Attota, R. M. Silver, M. Bishop, E. Marx, J. Jun, M. Stocker, M. Davidson, and R. Larrabee, "Evaluation of new in-chip and arrayed line overlay target designs," Proc. SPIE, **5375**, 395 (2004).
16. R.M. Silver, R. Attota, M. Stocker, M. Bishop, J. Jun, E. Marx, M. Davidson, and R. Larrabee, "High resolution optical overlay metrology," Proc. SPIE **5375**, 78 (2004).
17. R. Attota, R.M. Silver, T.A. Germer, M. Bishop, R. Larrabee, M.T. Stocker, and L. Howard, "Application of through-focus focus-metric analysis in high resolution optical metrology" Proc. SPIE, **5752**, 1441-1449 (2005).
18. R. Attota, R.M. Silver, and J. Potzick, "Optical illumination and critical dimension analysis using the through-focus focus metric method," Proc. of SPIE **6289** 62890Q-1 (2006).
19. H.F. Talbot, "Facts relating to optical science no. IV," Phil. Mag. **9** (1836).

1. Introduction

In the majority of optical microscopes emphasis is given to achieve uniform spatial irradiance at the sample plane using the Köhler illumination configuration [1-2]. In this configuration, the illumination source is mapped onto the back focal plane. Each point on the back focal plane uniformly illuminates the sample plane. This scheme essentially neutralizes source intensity non-uniformities and produces spatially uniform irradiance at the sample. This is usually sufficient for general microscopy. However, for three-dimensional objects, obtaining Köhler illumination with homogenous spatial irradiance is necessary, but not sufficient. It is also necessary to achieve angular illumination symmetry. This is critical for high precision metrology applications, where illumination asymmetry results in varied partial coherence as a function of field position, resulting in changes in line width (CD) across the field [3, 4]. In other words, angular illumination asymmetry results in a distorted optical irradiance profile and will potentially lead to errors in measurements or lithographic exposure.

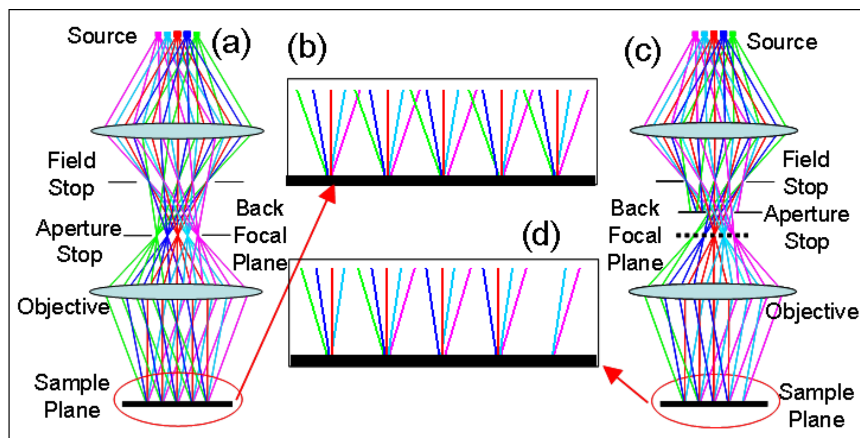

Fig. 1. (a) A simplified schematic of Köhler illumination for reflection microscope with the aperture stop at the back focal plane. (b) Homogeneous angular illumination at the sample plane for (a). (c) Kohler illumination with aperture stop displaced axially and radially from the back focal plane. (d) Inhomogeneous angular illumination at the sample plane for (c).

Several direct and indirect methods related to illumination analysis are available in the literature [5-12], including optical lithography stepper and scanner applications. Methods

used include a pinhole camera, grating pinhole camera, linear phase grating, and source metrology instrumentation for illumination analysis with a final goal of determining illumination uniformity at the aperture stop (pupil plane). Illumination inhomogeneity at the aperture stop directly results in angular illumination asymmetry at the sample plane. In this paper, a novel method to measure angular illumination asymmetry (ANILAS) directly at the sample plane (field plane) of optical microscopes by using a set of through-focus optical images is presented. The proposed method has the potential advantages of low cost, high speed, and simplicity, and does not require modifications to the optics. Sohn et al. [11] proposed Kohler Factor 2 (KF2) for angular illumination homogeneity, whereas ANILAS indicates angular illumination asymmetry.

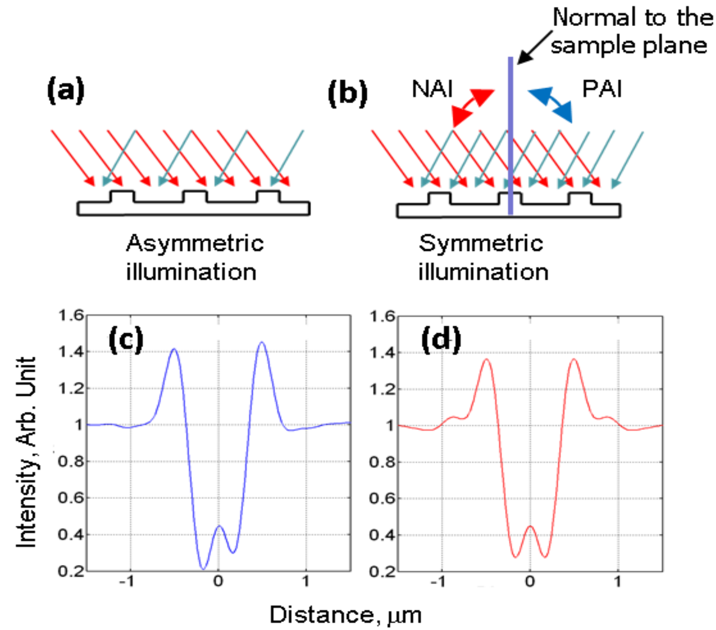

Fig. 2. Schematic representation of (a) Asymmetric and (b) Symmetric angular illumination conditions. Simulated intensity profiles of an isolated line for (c) Asymmetric and (d) Symmetric illuminations. NAI = negative angles of illumination, PAI = positive angles of illumination, Line width=200 nm, Line height=200 nm, Illumination NA=0.4, collection NA=0.8, Wavelength=546 nm, and Si line on Si substrate.

2. Effect of ANILAS

In this section, the influence of ANILAS on the formation of optical images is described. In an optical microscope designed for Köhler illumination (Figs. 1(a) and (c)), the illumination source is imaged at the back focal plane of the objective. Each point at the back focal plane (or at a conjugate back focal plane) produces an illumination plane wave on the target at the corresponding specific illumination angle. Aggregate spatial irradiance at the field plane is the addition of radiant intensity produced by all the angles of illuminations. For this reason, projected illumination irradiance at the field plane is spatially uniform and thus nullifies the inhomogeneity in the source illumination (Fig. 1(b)) [1, 2].

For an ideal optical microscope, (i) illumination angles are symmetric to the optical axis, and (ii) the radiant intensity of any two symmetrically opposite illumination angles are the

same. However, there could be deviations from this ideal illumination. This is illustrated in Fig. 2 using two variations of illumination. For the sake of simplicity, only two symmetrically opposite illumination planes are shown in the figure. The symmetrically opposite illumination directions can have different or equal irradiances as shown in Fig. 2(a) and (b), respectively. Both of the illumination schemes produce uniform magnitude of irradiance across the field of view (FOV). However, the illumination scheme in Fig. 2(a) has asymmetric angular illumination. As expected, the simulated optical images (using a rigorous coupled wave-guide analysis model (13)) for this asymmetric illumination produced an asymmetric profile for a Si line protruding from a Si substrate (a three-dimensional object) as shown in Fig. 2(c), while the symmetric illumination produced a symmetric profile as shown in Fig. 2(d). It can be expected that asymmetric illumination results in inaccurate measurement results. Therefore, it is critical to obtain symmetric angular illumination for high precision applications of optical tools, in addition to spatially uniform irradiance. Evaluating ANILAS is the first step.

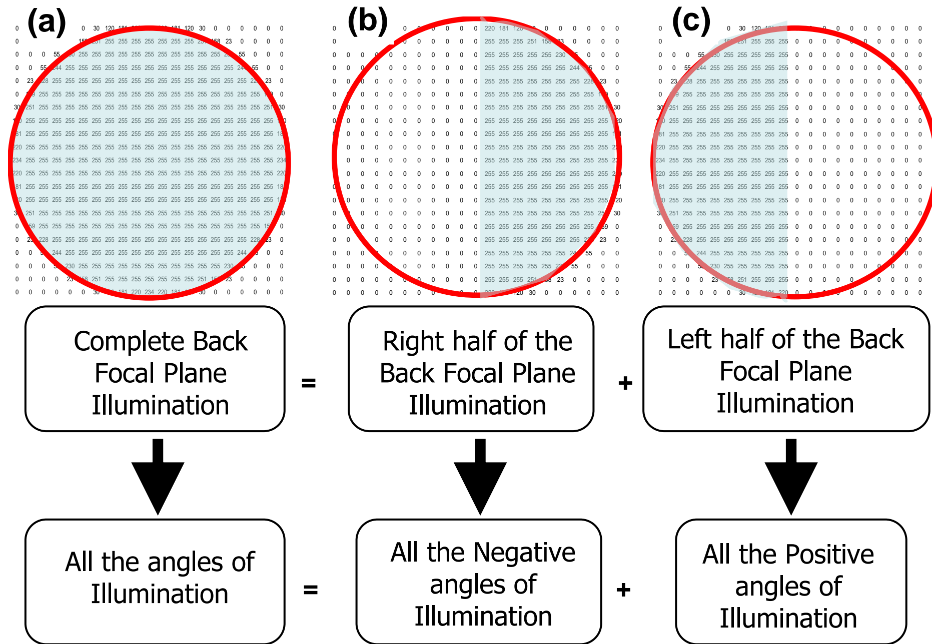

Fig. 3. Back focal plane intensity is represented by a matrix of numbers in the simulations. Simulations were made using three fill factors at the back focal plane. (a) Complete circular, (b) right semicircular and (c) left semicircular fill factors.

3. ANILAS analysis

For an incoherent light source (in an optical microscope), each individual plane wave independently illuminates a target and produces an image. The final image is the incoherent sum of all the individual images formed by all the illuminating plane waves [14]. For ANILAS analysis, the Köhler illumination is divided in the following way. All the angles of illumination to the right and the left of the normal to the sample plane are bundled into positive (PAI) and negative (NAI) angles of illumination, respectively (Fig. 2(b)). The total illumination at any location is the sum of all of the PAI and the NAI. This implies that the final image is formed by incoherently adding the images formed by all of the NAI and the PAI.

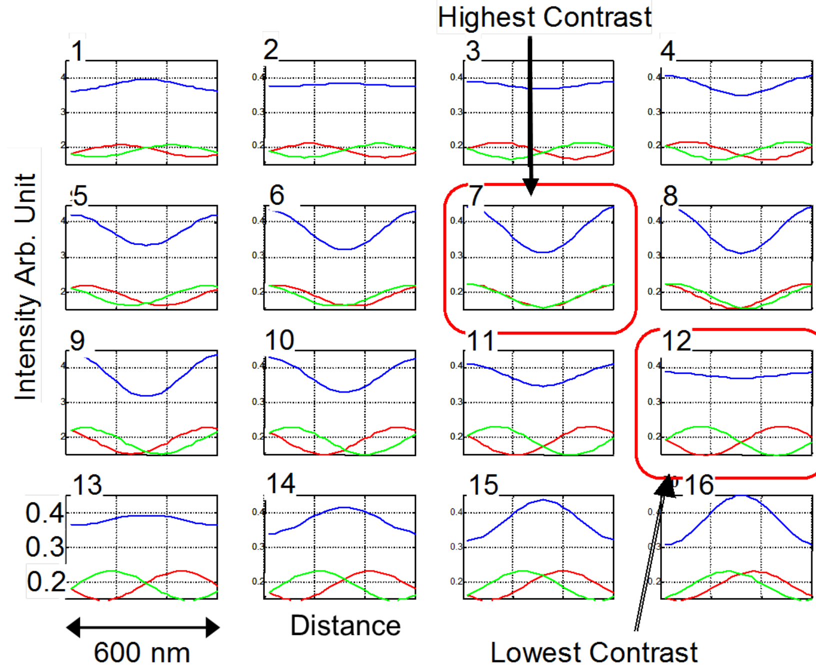

Fig. 4. Simulated through-focus image intensity profiles of a line grating. The lower overlapping curves in each window are the intensity profiles for only negative and positive angles of illuminations. The above curve is the intensity profile for all the angles of illumination. Each window is at a different focus position with a focus step height of 200 nm. X (0 nm to 600 nm) and Y (0 to 0.5) axes scales are kept constant for all the windows. The profile of only one pitch is shown in the figure. Input parameters for the simulation: Line width = 200 nm, Line height = 200 nm, Pitch = 600 nm, Illumination NA = 0.4, Collection NA = 0.8, Illum. Wavelength = 546 nm, Si line on Si substrate.

Using this division of illumination, the image formation of a line grating target as it is scanned through the focus using the rigorous coupled wave guide (RCWA) optical simulation model [13] is studied. In the RCWA model, the illumination at the back focal plane is represented by a matrix of numbers that fill or tile a circle as shown in Fig. 3. Each number in the circular matrix produces an illumination plane wave at its corresponding angle of incidence. The magnitude of the number determines the intensity of the illuminating plane wave. For this simulation study, the sample plane normal coincides with the optical axis. The simulated images for three sets of values of back focal plane fill factors were analyzed. In the first type of illumination, the circular back focal plane was illuminated with uniform intensity. This resulted in all the angles of illumination having equal projected radiant intensity on the target. In the second type of fill factor, only the right half of the back focal plane was uniformly illuminated, resulting in only the PAI. In the third type, only the left half of the back focal plane was uniformly illuminated resulting in only the NAI. The through–focus image intensity profiles for the three types of illuminations are shown in Fig. 4.

The following observations can be made from this result. Irradiance profiles formed by only the NAI or only the PAI appear different. Their shapes change with focus position. The final image formed from all the incident angles is the incoherent sum of the images formed from only the NAI and from only the PAI. When the maximum and the minimum irradiances of the images formed by only the NAI and only the PAI align (or are in phase), the resultant

final image has the highest contrast (window 7 in Fig. 4). Window 12 shows the instance where there is out-of-phase overlap in the peak values, resulting in the lowest-contrast final image. The images formed from only the negative or only the positive angles of illumination by themselves do not produce the low contrast final images. However, when the irradiances are added, they produce the low or high contrast final image. Because of the way negative and positive illumination profiles add up, the contrast in the final image cyclically increases and decreases several times as the focus height is scanned.

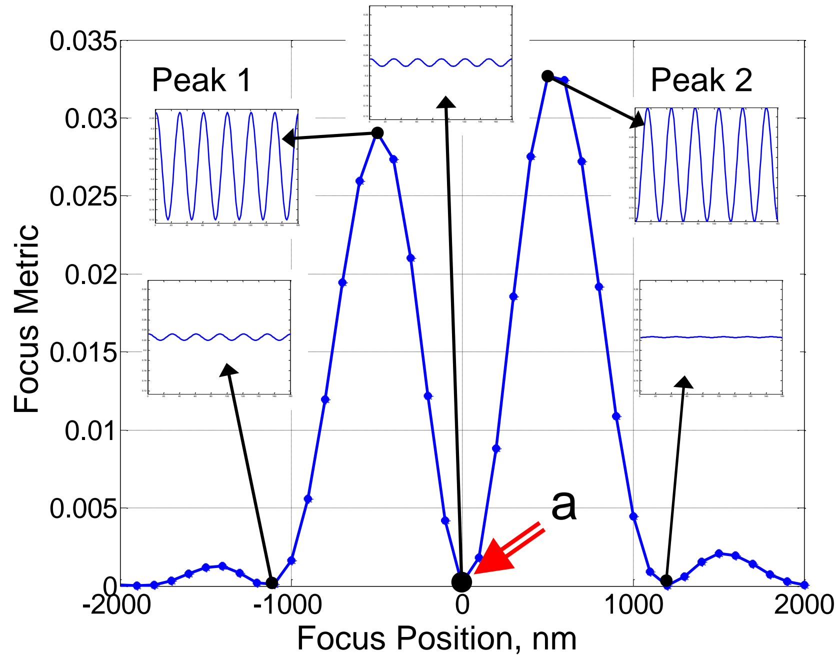

Fig. 5. A typical simulated focus metric (FM) signature for line array exhibiting proximity effects. Insets are intensity profiles at the indicated focus positions. The optical image has high contrast at peaks 1 and 2, while it has very low contrast at point "a" as shown by an arrow. Parameters for the simulation: Line width=140 nm, Line height=200 nm, Pitch=600 nm, Illumination NA =0.4, NA=0.8, Wavelength=546 nm. Si lines on Si substrate. Zero position represents top of the substrate.

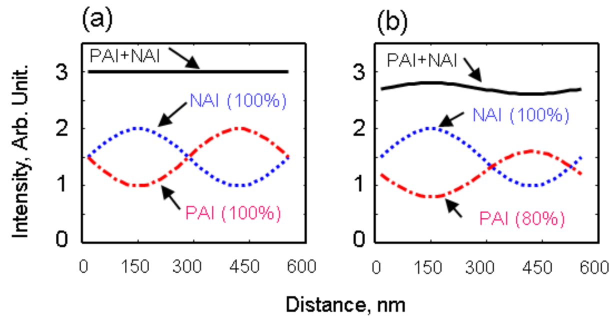

Fig. 6. Schematic intensity profiles for the NAI, the PAI, and all the angles of illumination at the focus position "a" (in Fig. 5). Percentage of the left-half intensity compared to the right half is indicated in the figure. Length of the profile equals to one pitch.

This cyclical behavior can be studied using a metric called the 'focus metric' (FM) [15-18]. The FM is defined here as the sum of the mean square slopes of the irradiances in an optical image. A plot of the FM as the target moves through-focus is defined as the FM signature. The FM signature typically has a single peak when imaging a target. The image at the peak of the FM signature is usually considered to be the image at the best focus position. However, under certain conditions, the FM signature of a line grating produces multiple FM signature peaks as shown in Fig. 5 [15-18]. The original work of Talbot reported similar appearing and disappearing line profiles as a function of focus position [19]. Because of the high contrast of the final images at peaks 1 and 2, they have the high FM values. In the same way, because of the low contrast of the final image at the valley point "a," the FM value is nearly zero.

The example shown in Fig. 4 also exhibits a similar FM signature with multiple peaks. The window 12 image focus position in Fig. 4 corresponds to point "a" in Fig. 5. By moving the sample focus position in small incremental steps, a certain point is reached at point "a," where the sum of the images formed by the NAI and the PAI produces an almost constant intensity, lowest contrast image, and hence has a nearly zero FM value. Further examination of the images at this focus position provides additional insight into the illumination condition.

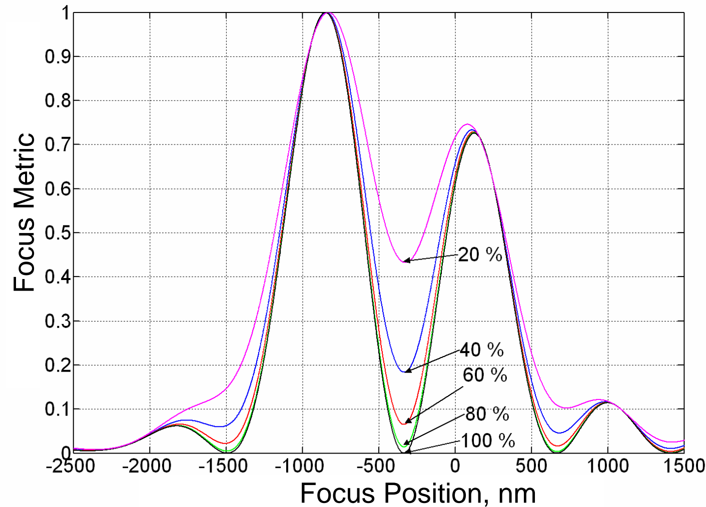

Fig. 7. The FM signatures with reduced right-half back focal plane intensity. Percentage of the right-half intensity compared to the left half is indicated in the figure.

Uniform illumination of the entire back focal plane (NAI=PAI) produces a constant irradiance profile schematically shown in Fig. 6(a). The focus metric has near zero value. However, when the intensity of all the PAI is uniformly reduced to, for example, 80 % of the NAI, the incoherent sum of the profiles no longer produces a constant irradiance profile as shown in Fig. 6(b). This results in a slightly higher contrast final image at point "a." Further reduction of the intensity of all the PAI uniformly continues to increase the contrast of the final image. This analysis shows that increasing the irradiance differences between the NAI and the PAI increases the FM value at point "a" (Fig. 5). Consequently, it can be observed that the FM value at the valley point "a" increases with an increasing difference in the magnitudes of NAI and the PAI irradiances; i.e. contrast at point "a" increases with increasing angular illumination asymmetry. The simulated FM signatures using the different degrees of ANILAS are shown in Fig. 7. As expected, the FM value at point "a" increased with

increasing irradiance difference. Hence, it can be concluded that the value of FM at point "a" indicates ANILAS at the location of analysis in the FOV. Evaluating FM values (at point "a") across the FOV and plotting their values at their corresponding location results in an ANILAS map and provides a convenient way of assessing the illumination condition at any location in the FOV.

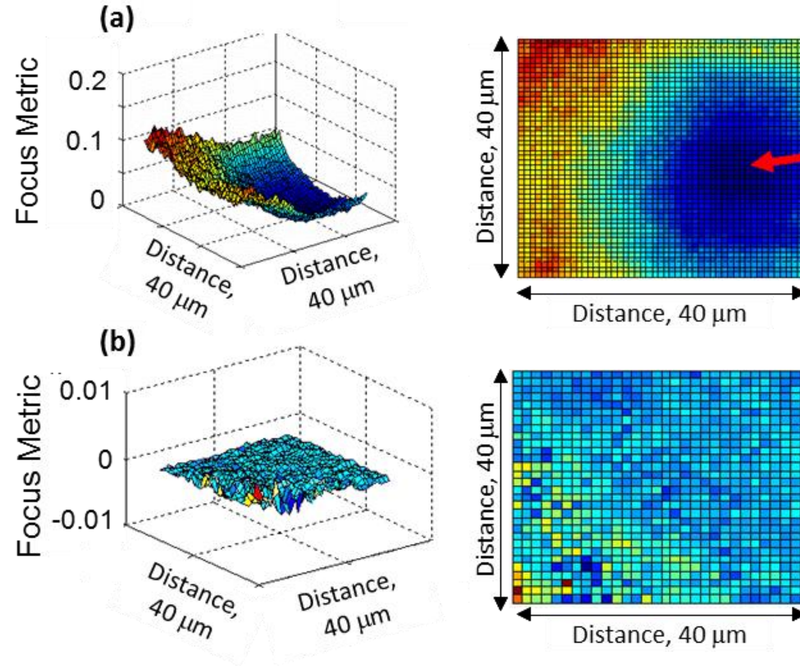

Fig. 8. The experimental evaluation of the illumination (ANILAS). The right-side figure is a two-dimensional projection of the left-side three-dimensional figure. (a) Poorly aligned microscope and (b) Well aligned microscope. X and Y are distance axes representing 40 µm of the field of view in both (a) and (b).

4. Experimental evaluation of ANILAS map

Based on this observation, an experimental illumination analysis was done for two microscope alignment states. In the well-aligned microscope, the aperture stop is centered at the back focal plane resulting in homogeneous angular illumination (Figs. 1(a) and 1(b)). While, in the poorly aligned setup, the aperture stop was displaced axially and radially from the correct back focal plane location, resulting in inhomogeneous illumination (Figs. 1 (c) and 1(d)). With these alignments, through-focus images of a line grating were acquired in two perpendicular target orientations. In the analysis, the entire field of view was divided into a grid of N rows and M columns, and the FM signatures were calculated for each sub field. The resulting normalized minimum focus metric values at point "a" were obtained for each of the M x N sub field locations for the two perpendicular orientations. A plot of the resultant minimum FM values across the field of view shows the asymmetry in the angular illumination.

The experimental results for the poorly aligned microscope are presented in Fig. 8(a). In the three-dimensional image on the left side, the x-y axes represent the FOV and the z-axis represents the magnitude of the FM value at point "a." The results show that the poorly

aligned microscope has large angular illumination asymmetry across the field of view, as illustrated in Figs. 1(c) and 1(d). For this configuration of the microscope, an arrow shows the location in the field of view with the lowest value of the FM. Based on the discussion above, this location in the field of view for this microscope setup should show the best angular illumination symmetry; i.e. an image of a symmetric line at this location should produce the best symmetric profile. The asymmetry in the illumination increases further one moves away from the location of best symmetry. Figure 9 shows experimental verification of the above generated ANILAS maps. For the poorly aligned microscope, it shows symmetric line profiles only at the location indicated with an arrow mark, as evaluated by the ANILAS method. The well-aligned microscope has much lower ANILAS, as shown in Fig. 8(b). However, even this microscope setup has some angular asymmetry at the lower left corner of the FOV.

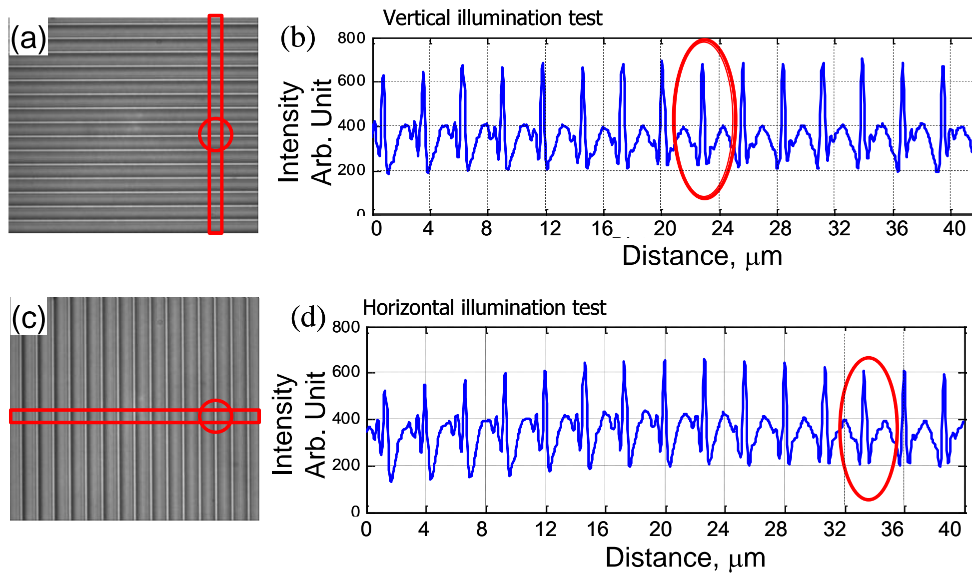

Fig. 9. Experimental verification of the ANILAS map for the poorly aligned microscope. (a) and (c) are the optical images of the horizontal and the vertical line gratings, respectively. (b) and (d) are the intensity profiles at the locations shown by rectangles in (a) and (c). Red circles / ellipses represent the location of best symmetry and agrees with the analysis shown in Fig. 8(a).

For this method to work, it is essential to select experimental conditions that produce an FM curve similar to the one shown in Fig. 5. A suitable combination of grating pitch, wavelength, illumination numerical aperture, and collection numerical aperture produces this type of FM curve [15].

At this initial stage, for the lack of a better metric, the FM value (at point “a”) as defined in the above procedure is proposed as the value of the ANILAS. A zero value of ANILAS across the FOV represents an ideal microscope with no asymmetries in the illumination and is best suited for critical applications such as metrology and lithography. Deviations from this ideal illumination can have several variations, one of which can be as shown in Fig. 8(a), in which there is also a near zero ANILAS value, but only at the location shown by the arrow mark.

At this time, the smallest value of ANILAS that can be detected (sensitivity) is not known, and hence further work is needed. Also not fully understood are all of the possible parameters or conditions that affect the ANILAS map. However, the proposed ANILAS map for a microscope is expected to provide a useful method for assessing illumination conditions, which is especially needed for critical measurements. The procedure is simple, inexpensive, fast, and makes frequent analysis a possibility.

5. Summary

A line grating, under certain conditions, produces multiple cycles of increased and decreased contrast as a function of focus position. A plot of the image contrast (FM value) with focus position produces multiple peaks. The value of FM at the valley (between two FM peaks) depends on the angular illumination asymmetry (ANILAS). Based on this, a new method to evaluate ANILAS has been proposed. A plot of ANILAS across the field of view of an optical microscope generates an ANILAS map for that microscope condition that is expected to provide a useful method of assessing the illumination condition. A theoretical explanation and an experimental verification of the same have been presented.

Acknowledgements

The authors would like to thank Yeung-Joon Sohn, for the helpful discussions and Bryan Barnes, and Mike Stocker for their generous assistance in the laboratory equipment. The authors also thank SEMATECH for providing the line grating sample.